JACS
JOURNAL OF THE AMERICAN CHEMICAL SOCIETY

ARTICLE

pubs.acs.org/JACS

High Performance Weak Donor−Acceptor Polymers in Thin Film Transistors: Effect of the Acceptor on Electronic Properties, Ambipolar Conductivity, Mobility, and Thermal Stability

Jonathan D. Yuen,[†,∥] Jian Fan,[†,§,∥] Jason Seifter,[†] Bogyu Lim,[†,‡] Ryan Hufschmid,[§] Alan J. Heeger,*[,†,§] and Fred Wudl*[,†,§]

[†]Center for Polymers and Organic Solids, University of California, Santa Barbara, California 93106, United States

[‡]Center for Advanced Molecular Photovoltaics, Stanford University, Stanford, California 94305, United States

[§]Center for Energy Efficient Materials, University of California, Santa Barbara, California 93106, United States

Supporting Information

ABSTRACT: We have studied the electronic, physical, and transistor properties of a family of donor−acceptor polymers consisting of diketopyrrolopyrrole (DPP) coupled with different accepting companion units in order to determine the effects of donor−acceptor interaction. Using the electronically neutral benzene (B), the weakly accepting benzothiadiazole (BT), and the strongly accepting benzobisthiadiazole (BBT), the accepting strength of the companion unit was systematically modulated. All polymers exhibited excellent transistor performance, with mobilities above 0.1 $cm^2V^{-1}s^{-1}$, even exceeding 1 $cm^2V^{-1}s^{-1}$ for one of the BBT-containing polymers. We find that the BBT is the strongest acceptor, enabling the BBT-containing polymers to be strongly ambipolar. The BBT moiety also strengthens interchain interactions, which provides higher thermal stability and performance for transistors with BBT-containing polymers as the active layer.

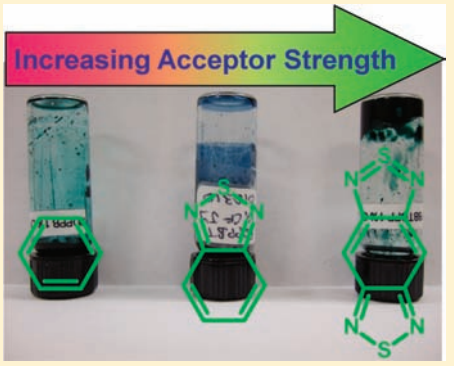

INTRODUCTION

While initially conceived toward the development of conjugated polymers with tailored electro-optical properties for photovoltaic applications,[1] the maturation of the donor−acceptor (DA) copolymer approach has also led to the extension of DA polymers to thin film transistor (TFT) applications. Progress in DA polymers as active layers for TFTs has yielded materials with mobilities consistently exceeding 0.1 $cm^2V^{-1}s^{-1}$.[2] Even more significant are recent reports of DA polymers with TFT mobilities nearing or surpassing 1 $cm^2V^{-1}s^{-1}$,[3] with performance comparable to those of amorphous silicon TFTs. Combined with other attractive physical properties such as good solution processability, mechanical flexibility and compatibility with thermally sensitive flexible substrates, DA polymers now appear to be strong candidates as active layers for low-cost and flexible electronics.[4]

DA polymers consist of a combination of π-electron rich and π-electron deficient conjugated moieties (donors and acceptors, respectively) arrayed along the polymer chain, which determines the electronic behavior of the resulting polymer. While p-type (hole transport) behavior has been observed in almost all DA polymers, robust n-type (electron transport) or ambipolar (coexistent hole and electron transport) behavior is dependent on the type of acceptor used.[5] The exact role the acceptor moiety plays in n-type transport is unclear and thus a subject worthy of study. To illustrate, we describe and compare two acceptor moieties that are currently the focus of our research, diketopyrrolopyrrole (DPP) and benzobisthiadiazole (BBT), shown in Figure 1a. We have previously synthesized a family of DA polymers with BBT as the acceptor moiety,[6] observing that ambipolar behavior is universal for these polymers. Interestingly, in contrast to BBT, n-type behavior is not universal in polymers with DPP as the accepting moiety. While many DPP-containing polymers exhibit ambipolar behavior,[7] just as many show only p-type behavior.[8]

The integration of DPP into high performance polymers has been extensively reported, with many DPP-containing polymers exhibiting mobilities from 0.1 $cm^2V^{-1}s^{-1}$ up to 1 $cm^2V^{-1}s^{-1}$. We are therefore interested in harnessing the high performance effect of DPP in transistor fabrication. However, in the present study, instead of using a strong electron donor (such as thiophene containing monomers) to couple to DPP, we decided to couple DPP with different acceptor units, such as BBT. In order to observe the interaction between DPP and its companion accepting unit, the accepting strength of the companion unit was systematically modulated through chemical modification. As shown in the top section of Figure 1a, this can be achieved by starting out with BBT and then using monomers with increasingly less thiadiazole units attached. With one less thiadiazole unit, a weaker accepting benzothiadiazaole (BT) is formed, and with no thiadiazole units, we have an electronically neutral

Received: June 17, 2011
Published: November 01, 2011

dx.doi.org/10.1021/ja205566w | J. Am. Chem. Soc. 2011, 133, 20799–20807

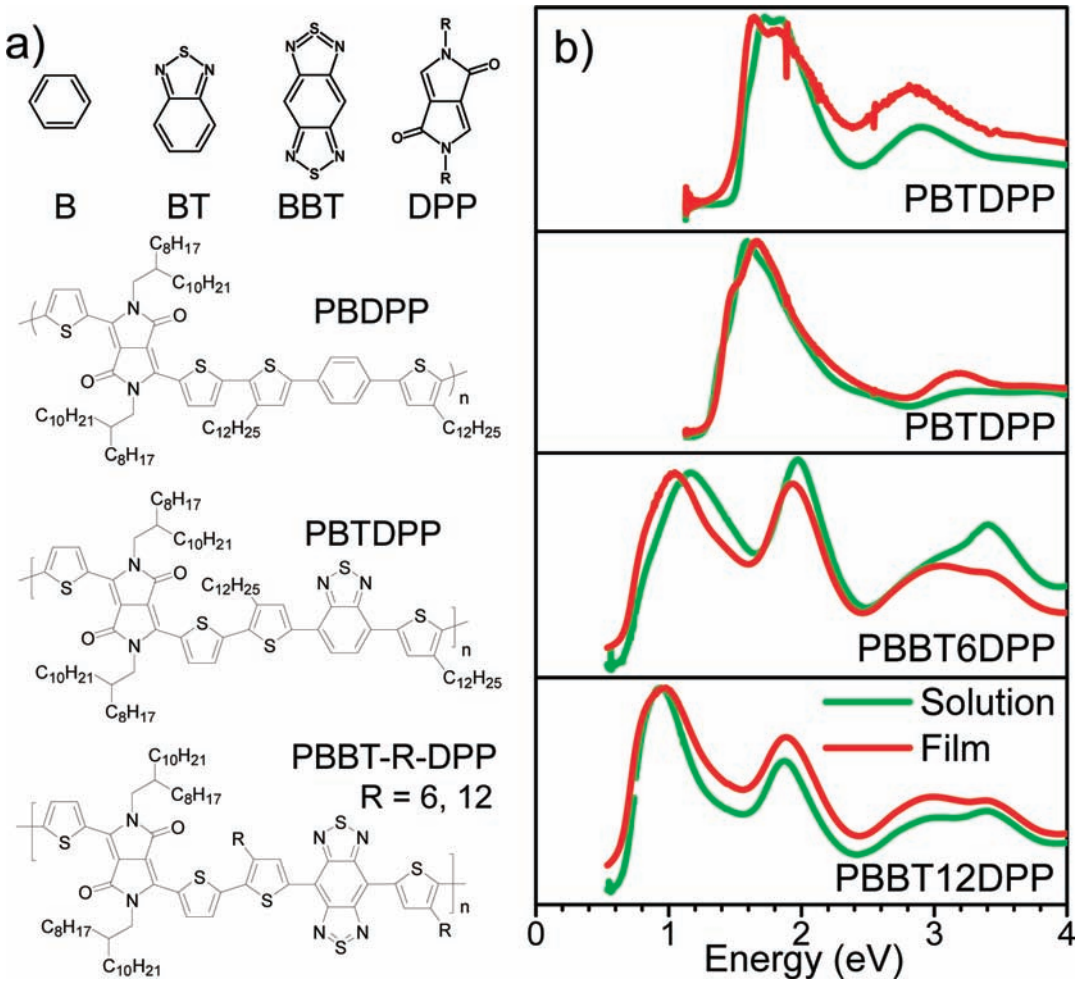

Figure 1. (a) Chemical structures of the accepting moieties used (top) and the resulting polymers synthesized (bottom). (b) UV-vis-NIR spectra of the polymers in both film and solution.

benzene (B). Since the modulation of the thiadiazole unit(s) occurs perpendicularly to the polymer chain, the electronic properties can be varied without any change in either the backbone structure of the repeat unit or the solublizing side groups that decorate the repeat unit. This procedure effectively allows us to control the effects of the solubilizing side groups and the length of the repeat units, as they remain unchanged between the polymers. In subsequent sections of this report, we describe and compare the electronic properties of DPP-containing polymers synthesized with B, BT, or BBT, and show how the interactions between these moieties determine device behavior when the polymers are used as TFT active layers.

RESULTS

Synthesis of Polymers. PBDPP, PBTDPP, PBBT6DPP, and PBBT12DPP (shown in the lower portion of Figure 1a) were synthesized via Suzuki coupling between DPP-dithiophene boronic acid pinacol ester (DPPDT) and the dibrominated dithiophene-accepting moiety (BDT, BTDT, BBTDT6 or BBTDT12) as shown in Figure S1 in the Supporting Information (SI). A more detailed description of the syntheses is also available in the SI. The monomer BBTDT was found to be rather difficult to solublize and so hexyl and dodecyl side groups were attached to dithiophene units, resulting in BBTDT6 or BBTDT12, respectively. The number average molecular weights and polydispersity indices, as listed in Table 1, are derived using gel-permeation chromotogaphy (GPC). GPC measurements were carried out for all polymers in 1,2,4-trichlorobenzene (TCB) at 150 °C. It was found that the molecular weights of PBTDPP, PBBT6DPP, and PBBT12DPP were similar, but for PBDPP, the molecular weight was more than double compared to those of the others. Measurements for PBTDPP and PBDPP were also carried out in chloroform (CF) at room temperature and the data is available in the experimental section of the SI, along with the GPC traces for all measurements. The measured molecular weights for PBDPP and PBTDPP were substantially less in hot TCB than in chloroform, most probably due to aggregation of the polymers in chloroform.

Optical and Electronic Properties. As shown in Figure 1b, the UV-vis-IR spectra of all four polymers, both in ortho-dichlorobenzene/chloroform and in film are classified by polymer type. The bandgaps of the four polymers, derived from the spectra, are summarized in Table 1. We observed that the integration of BBT typically results in polymers with very low bandgaps of below 1 eV.[9] PBBT6DPP and PBBT12DPP are no exceptions, with both polymers having very narrow bandgaps of around 0.65 eV. We observed that for PBBT6DPP and PBBT12DPP, the change in solublizing side groups does not strongly affect the electronic properties of the polymer. In contrast,

Table 1. Energy Levels for the DPP-Based Polymers Studied and Their Constituent Monomers: Optical Energy Gap (E_g), HOMO Levels and LUMO Levels As Derived from Cyclic Voltammetry and Absorption Measurements[a]

name	PBDPP	PBTDPP	PBBT6DPP	PBBT12DPP	DPPDT	BDT	BTDT	BBTDT
E_g (eV)	1.5	1.35	0.65	0.65	1.9	3.2	2.1	1.6
HOMO (eV)	−4.7	−4.75	−4.55	−4.55	−5.3	−5.5	−5.2	−5.4
LUMO (eV)	−3.2	−3.4	−3.9	−3.9	−3.4	−2.3	−3.1	−3.8
M_n (kD)/PDI	21/2.1	9.4/1.6	8.7/1.5	8.8/1.8	N/A	N/A	N/A	N/A

[a] Physical properties of the DPP-based polymers; number molecular weight (M_n) and polydispersity index (PDI) are also listed.

variations in the acceptor strength of the companion moieties result in significant changes, with the bandgap of the resulting polymer increasing with decreasing acceptor strength. Thus, for PBTDPP and PBDPP, their bandgaps increase to 1.35 eV and 1.5 eV, respectively. It is interesting to note that there is only a slight drop in bandgap of 0.15 eV from PBDPP to PBTDPP. In contrast, there is a significant drop of almost 1 eV in bandgaps for the BBT-containing polymers compared to PBTDPP.

This difference in drop in bandgap can be explained by comparing the energy levels of the different polymers, and also with those of the constituent monomers. The comparisons are summarized in Table 1. The energy level with respect to the vacuum level of the lowest unoccupied molecular orbital (LUMO) for each material was derived from cyclic voltammetry (CV) where LUMO = 4.8 eV − ΔE. ΔE is calculated by measuring the difference between the onset of reduction and the half-wave potential of the ferrocene standard. The highest occupied molecular orbital (HOMO) level was derived from the difference between the LUMO level and the optical bandgap, that is, HOMO = LUMO + optical bandgap. The reverse was applied to BDT as the reduction point could not be observed, where HOMO = 4.8 eV + ΔE. ΔE is calculated by measuring the difference between the onset of oxidation and the half-wave potential of the ferrocene standard. The LUMO level was derived from the difference between the HOMO level and the optical bandgap, that is, LUMO = HOMO−optical bandgap.

The most striking observation we made is how significantly the LUMO level of the resulting polymer was determined by the LUMO level of its stronger accepting moiety. For PBBT6DPP and PBBT12DPP which had LUMO levels of −3.9 eV, the LUMO level of each polymer was determined by the LUMO level of its respective constituent BBTDT monomer, which was around −3.8 eV. In the case of both PBTDPP and PBDPP, DPPDT was the determining moiety, with LUMO levels between −3.2 eV and −3.4 eV for both monomer and polymer. This explains the small difference in bandgap between PBTDPP and PBDPP, and why a sharp drop in bandgap is observed for the BBT-containing polymers compared to the other polymers.

The effect of the constituent monomers on the HOMO levels of the resultant polymers was more complex. For all the polymers, the HOMO level was moved substantially below the vacuum level, −4.55 to −4.75 eV as compared to between −5.2 and −5.5 eV for the monomers. This phenomenon can be somewhat accounted for by DFT calculations performed by Bredas et al.[10] on BBT-containing oligomers of differing lengths. It was found that as the oligomer length increased, a significant decrease in the magnitude of the HOMO level, compared to that of a single monomer, occurred. This decrease was such that upon extrapolation, a polymer of infinite length would have a HOMO level reduced by 1 eV, close to what we observed for the BBT-containing polymers. We believe that the same can be applied to PBDPP and PBTDPP, as the thiadiazole units did not significantly affect the HOMO levels of all the monomers, as compared to the LUMO levels.

Therefore, we find that the categorization of "donor" and "acceptor" moieties is not entirely definitive. Interacting moieties will take on donor and/or acceptor roles depending on their relative energy levels. For PBDPP and PBTDPP, the role of the acceptor is taken up by the DPP moiety and the resulting LUMOs are close to that of the original DPPBT monomer. In contrast, the BBT moiety is the acceptor for the BBT-containing polymers and these polymers have LUMOs of around −3.9 eV, close to that of BBTDT.

Polymer Thermal Properties. To determine the effect of the companion moiety on the thermal properties of the resulting polymers, differential scanning calorimetery and thermogravimetric analysis were performed on all polymers. The variation of the companion moiety does not significantly affect the chemical stability of all the polymers as shown by TGA (Figure S2 in the SI). We observed that detectable chemical degradation occurs only above 350 °C for all the polymers.

In contrast, differences were observed when DSC was used to determine the thermal transitions for each polymer. For all polymers, DSC scans were performed from room temperature up to a temperature below the decomposition point of each polymer (Figure S3 in the SI). For PBDPP and PBTDPP, endothermic transitions were observed during the first heating scan, with the onset for the endotherms occurring after 200 °C for both polymers and the end occurring at 265 °C for PBDPP and 295 °C for PBTDPP. No transitions were observed for both polymers for the second scan, implying a nontrivial thermal relaxation process. The DSC data indicates that a melting or chain relaxation process probably occurs for PBDPP and PBTDPP. In contrast, the inclusion of the BBT moiety results in a significant difference in thermal properties, as DSC scans of the BBT-containing polymers show no significant endothermic transitions.

Transistor Fabrication, Ambipolarity and Transistor Performance with Correlation to Polymer Film Behavior. We find that the electronic and thermal properties observed above play a large role in determining the transistor behavior of each polymer. To test transistor performance, bottom-gate, Au bottom-contact transistors were fabricated with all four polymers as the active layer on heavily doped silicon substrates. The insulator used was a 200 nm SiO_2 layer passivated with decyltrichlorosilane (DTS). A more detailed description of the fabrication process is available in the SI. The transistor samples were annealed at various temperatures each for 10 min in order to locate the optimal annealing temperature that would result in the highest performing devices. All devices were tested and annealed in nitrogen-purged gloveboxes. All samples measured had channel length of 5 μm and channel width of 1 mm. In terms of

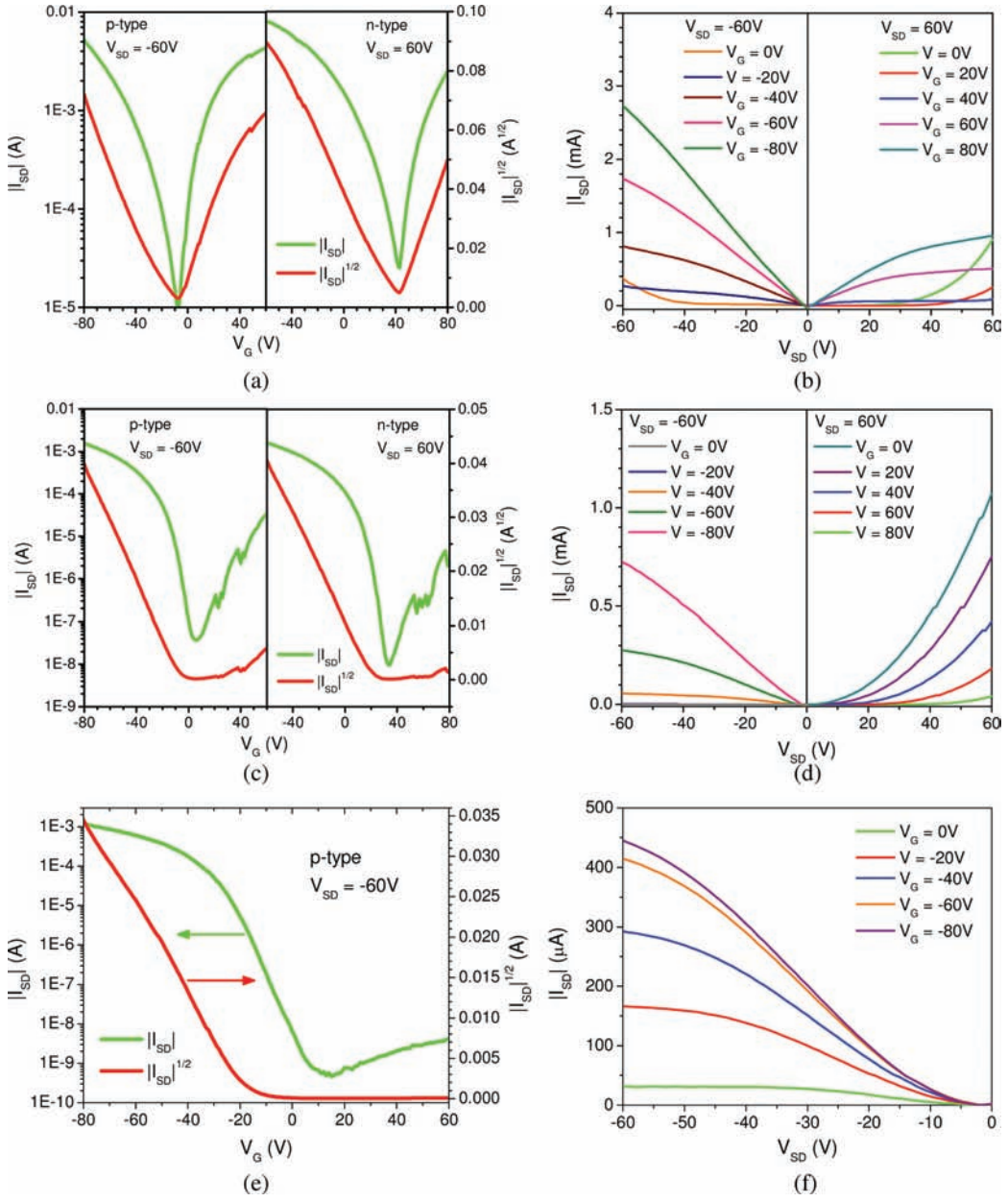

Figure 2. Typical transistor characteristics of PBBT12DPP, PBTDPP, and PBDPP at optimized annealing temperatures. 2a and 2b: Transfer and output characteristics, shown respectively, of a PBBT12DPP transistor annealed at 240 °C with mobilities determined to be 1.1 $cm^2V^{-1}s^{-1}$ for n-type transport and 1.0 $cm^2V^{-1}s^{-1}$ for p-type transport. 2c and 2d: Transfer and output characteristics, shown respectively, of a PBTDPP transistor annealed at 200 °C with p-type mobility determined to be 0.2 $cm^2V^{-1}s^{-1}$. 2e and 2f: Transfer and output characteristics, shown respectively, of a PBDPP transistor annealed at 160 °C with p-type mobility determined to be 0.17 $cm^2V^{-1}s^{-1}$.

processability, PBDPP and PBTDPP were more soluble than both BBT-containing polymers. Both PBDPP and PBTDPP dissolved within an hour of stirring in chloroform, whereas PBBT6DPP and PBBT12DPP required about 4 days of stirring in order to achieve the best transistor results, and even then, particles were still observed to cluster around the solution rim. In fact, solutions of PBBT12DPP left undisturbed resulted in the formation of inelastic gels. Photographs comparing the fluidity of solutions of PBDPP, PBTDPP, and PBBT12DPP are shown in Figure S4 in the SI.

For each polymer, the type of moiety used has a profound effect on the polarity of their transistor behavior. Figure 2 compares the performance of the polymers, with the transfer and output curves of typical devices of PBBTDPP (Figure 2 panels a and b, respectively), PBTDPP (Figure 2 panels c and d, respectively) and PBDPP (Figure 2 panels e and f, respectively) shown. In ambipolar TFTs[11] the transfer curves trace a V-shaped trough with decreasing magnitude of gate voltage, indicating a transition from unipolar to ambipolar behavior. This is reflected in the output plots exhibiting unipolar transport with standard linear-to-saturation current−voltage (IV) transistor characteristics at high gate voltages, and at low gate voltages, ambipolar transport with diode-like IV characteristics. This transition from the unipolar to ambipolar current regime means that a true 'off' state does not exist for ambipolar transistors. Hence, concepts such as on−off ratio or threshold voltage are difficult to apply.

dx.doi.org/10.1021/ja205566w |J. Am. Chem. Soc. 2011, 133, 20799–20807

This is in contrast to a bipolar transistor, in which unipolar n-type and p-type regimes exist, but not the coexistence of electrons and holes required for ambipolar transport. In the bipolar case, on−off ratios and threshold voltages can be determined for both n-type and p-type transport.

For ambipolar PBBT12DPP, equivalent n-type and p-type unipolar behavior can be clearly observed close to each other in both the transfer and output plots with maximum currents at $V_G = \pm 80$ V in the mA range. The inclusion of the BBT unit in the polymer results in a very narrow bandgap with high LUMO and HOMO energy levels which enable ease of injection for holes and electrons. Similar ambipolar transport behavior for PBBT6DPP TFTs can be observed in Figures S5a and S5b, available in the SI.

In contrast, the lower LUMO levels of PBDPP and PBTDPP result in higher injection barriers for electrons, and therefore, unipolar n-type transport cannot be observed in either PBDPP or PBTDPP transistors. PBDPP transistors exhibit pure unipolar p-type transport behavior in which large current is observed at strongly negative gate voltages, but negligible current is observed at strongly positive gate voltages. There is also a slight increase in current at strongly positive gate voltages due to leakage current. With the lack of the ambipolar current regime, it is relatively simple to determine on−off current ratios and threshold voltages. However, for PBTDPP, the transfer curves are V-shaped with slight current at positive gate and source-drain voltages. This is not due to gate leakage current. Rather it indicates a slight n-type injection that results in an ambipolar current contribution. However, this injection of n-type charges is not strong enough to sustain unipolar n-type operation as shown in the output curves. Nonetheless, transport characteristics for both polymers in the p-type unipolar regime are good, with output currents in the hundreds of μA to mA. Hence, by comparing the p-type and n-type transport for each polymer, we can observe that n-type transport behavior in DA polymers is strongly dependent on the strength of its acceptor.

It is interesting to compare the occurrence of ambipolarity in DPP-based polymers in literature to our polymers, particularly since high performance ambipolarity has been observed in polymers in which DPPDT has been directly coupled with B and BT,[7c,d] rather than BDT and BTDT. Comparing the LUMO levels determined by CV, we observe that PBDPP and PBTDPP have much lower LUMOs compared with many of the DPP-based polymers reported in literature,[7,8] including p-type only polymers. Therefore, it is expected that pure p-type or very weak ambipolarity can be observed in PDPPB and PDPPBT. More surprising is the number of DPP-based polymers which exhibit only p-type transport even though their LUMOs are comparable to the ambipolar ones.[8a,b] A review of the literature shows that high performance ambipolar transport is typically observed in DPP polymers in which the DPP units are separated from each other by only three aromatic cycles (or four cycles, if two of them are fused). N-type transport weakens as the number of electron donating aromatic cycles increases, sometimes becoming capable only of p-type transport. This process is clearly shown by comparing PBTDPP and PBDPP with the polymers synthesized with two less thiophene rings in the repeat unit. Exceptions are the BBT-containing polymers in this paper that show that the more strongly accepting BBT contributes greatly to the ambipolar behavior. This is unsurprising as high performance DPP-based dithienopyrrole[8b] and thienothiophene[8a] copolymers show only p-type transport or weak n-type transport. In contrast,

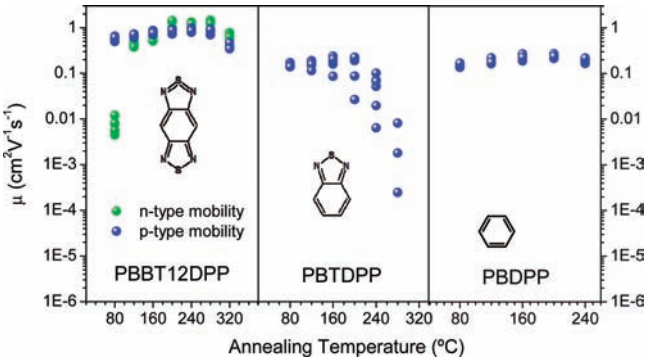

Figure 3. Transistor mobilities as a function of annealing temperature for PBBT12DPP (left), PBTDPP (center), and PBDPP (right). Six devices were tested for each material.

BBT-based dithienopyrrole[6,10] and thienothiophene[13] copolymers show strong ambipolarity.

To more accurately quantify and compare device performance, charge-carrier mobilities in the unipolar regimes were calculated using the standard equation used to describe MOS FETs operating in the saturation regime: $I_{DS} = {}^1/_2(W/L)\mu C_i(V_G - V_T)^2$, with mobility determined from $\partial|I_{DS}|^{1/2}/\partial V_G$. Mobilities as a function of annealing temperature for PBBT-12DPP, PBTDPP, and PBDPP are shown in Figure 3, with similar data for PBTT6DPP presented in SI Figure S3c. All devices were annealed prior to testing. It was found that an optimal annealing temperature, listed as T_o in Table 2, was required to achieve maximum mobility. However, for PBDPP and PBTDPP the variation in mobilities between 160 and 200 °C was so small that both values are cited. For each polymer, five to six devices were tested to observe sample-to-sample variations. By harnessing the high performance effect of DPP, all four polymers synthesized yielded optimal mobilities of over 0.1 $cm^2V^{-1}s^{-1}$. In particular, PBBT12DPP attained n-type and p-type mobilities of 1 $cm^2V^{-1}s^{-1}$ and beyond. Table 2 summarizes the average and maximum p-type (μ_h) and n-type (μ_e) mobilities for all the polymers at T_o, in addition to on−off ratios (I_{ON}/I_{OFF}) and threshold voltages (V_{TH}) for PBDPP. As noted above, the ambipolar regime prevents determination of either I_{ON}/I_{OFF} or V_{TH} values. Hence, they were not listed for PBTDPP, PBBT6DPP, and PBBT12DPP. We note that PBDPP and PBTDPP again are very similar, as T_o and mobilities are close to each other.

We found that the type of acceptor used has an influence on the TFT performance and thermal stability of the resulting polymer, with performance dependent on the thermal properties observed. As shown in Figure 3 and SI Figure S3c, the BBT-containing polymers follow similar trends to each other in transistor performance as a function of annealing temperature. The n-type and p-type mobilities of the polymers gradually increased over a wide temperature range, peaking at 240 °C, before rapidly decreasing at higher annealing temperatures. Nonetheless, we note the particularly high thermal stability, as n-type and p-type mobilities remained above 0.1 $cm^2V^{-1}s^{-1}$ from 100 °C up to 300 °C. By 340 °C, close to the degradation points of the polymers as shown by TGA measurements, no transport properties can be observed and a slight color change is observed in the film.

In contrast, the performance of PBDPP and PBTDPP is limited by the thermal transitions as observed in DSC measurements. From Figure 3, we see that PBTDPP and PBDPP also

Table 2. Transistor Performance Parameters—Optimized Annealing Temperature (T_o), Average Hole ($\mu_{h,avg}$) and Electron ($\mu_{e,avg}$) Mobilities and Maximum Hole ($\mu_{h,max}$) and Electron Mobilities ($\mu_{e,max}$) at the Optimized Annealing Temperature[a]

name	T_o (°C)	$\mu_{h,avg}$ ($cm^2V^{-1}s^{-1}$)	$\mu_{e,avg}$ ($cm^2V^{-1}s^{-1}$)	$\mu_{h,max}$ ($cm^2V^{-1}s^{-1}$)	$\mu_{e,max}$ ($cm^2V^{-1}s^{-1}$)	$I_{ON}/I_{OFF,\ Avg}$	$V_{TH,\ Avg}$
PBDPP	160/200	0.24/0.24	N/A	0.27/0.27	N/A	$10^6/10^6$	5/18
PBTDPP	160/200	0.17/0.16	N/A	0.23/0.23	N/A	N/A	N/A
PBBT6DPP	200	0.81	1.20	0.83	1.36	N/A	N/A
PBBT12DPP	240	0.89	0.99	1.17	1.32	N/A	N/A

[a] The average on-off ratios (I_{ON}/I_{OFF}, Avg) and threshold voltages (V_{TH}, Avg) for unipolar PBDPP are also listed.

exhibit mobility maxima with annealing temperature between 160 and 200 °C, far below those of the BBT-containing polymers. Moreover, we observed for PBDPP and PBTDPP that the maxima occurred around the onsets of the DSC endotherms. For PBTDPP, measurable transport ceased beyond 300 °C, coinciding with the end of the DSC endotherm and the polymer film visibly dewetting (last row of Figure S6 in the SI, which compares optical micrographs of the polymer films after various annealing temperatures). For PBDPP, the endotherm ended at around 260 °C, closely followed by the cessation of transport and the visible dewetting of the film when PBDPP transistors were annealed at 280 °C (last row of Figure S6 in the SI). As for PBBT12DPP, no such dewetting can be observed as shown in the last row of Figure S6 in the SI. Thus we conclude that the degradation in performance at lower annealing temperatures for both PBDPP and PBTDPP is caused by the loss in film coherence. In contrast, TGA data shows that the annealing temperatures associated with the cessation of transport for PBBT6DPP and PBBT12DPP approach those of the chemical degradation point of the polymers.

In addition to thermal stability, stability in the ambient is a great concern for polymer transistors in terms of commercialization. We have performed air-stability tests on transistors incorporating the highest performing material PBBT12DPP and found their behavior similar to those exhibited by PBBTPD transistors. In general, BBT-based polymers are readily doped in air. A description of the experiment is included in the SI. The air stability of PBBTPD with respect to transistor performance was described in a recent publication.[6] We found that while n-type transport is strongly affected, a protective layer of TiOX helps to extend the lifetime of the polymers.

Polymer Structural Properties. X-ray diffraction data provide further insight to the structural behavior of the polymers. Figure 4a shows the out-of-plane specular X-ray diffractograms (XRDs) taken at various temperatures for films of PBDPP, PBTDPP, and PBBT12DPP respectively. For better comparison, only the data for $2\theta = 3° - 6°$ is shown as measurements at higher angles did not show any defined diffraction peaks. In Figure 4a, diffractograms indicate that PBDPP has little or no out-of-plane ordering at all annealing temperatures, with no clearly defined peaks observed. In contrast, diffractograms for PBTDPP show intrinsic out-of-plane order already present in as-cast films of PBTDPP, with a peak centered around 3.6°. This corresponds to a separation length of around 2.5 nm, indicating the probable formation of a highly ordered lamellar structure with intersheet spacing equal to the separation length.[12] The formation of the lamellar structure implies that the chains are aligned edge-on with respect to the substrate. The peak is observed to strengthen up to around 240 °C and diminish as dewetting occurred. The additional peaks at 240 °C are associated with Kessig interference from surface reflections. For

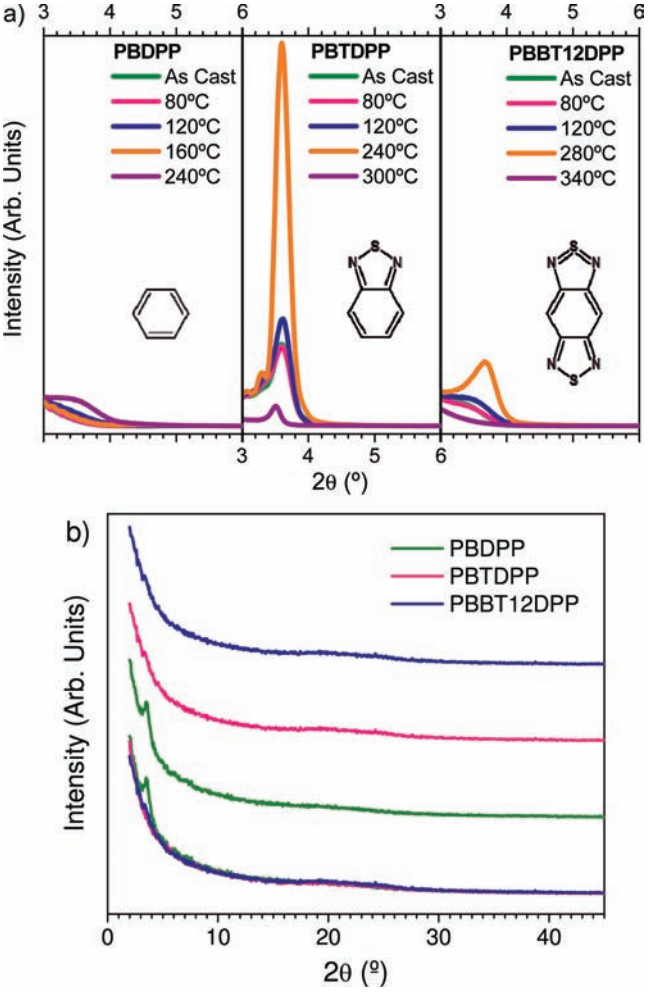

Figure 4. (a) Out-of-plane specular X-ray diffractograms for PBDPP (left), PBTDPP (middle), and PBBT12DPP (right) for various temperatures. (b) In-plane grazing incidence X-ray diffractogram for PBDPP, PBTDPP, and PBBT12DPP at optimized annealing temperatures.

PBBT12DPP, very broad and weak perturbations are observed in the diffractograms for samples annealed below 200 °C, indicating the occurrence of some ordering. For the film annealed at 280 °C, more ordering occurred such that a broad peak appears around 3.7°, indicating lamellae formation with an intersheet spacing of around 2.4 nm. We conclude that PBDPP has no out-of-plane order and that PBBT12DPP has less out-of-plane order than PBTDPP.

For each polymer, in-plane ordering was determined via in-plane grazing incidence XRD for PBDPP, PBTDPP, and PBBT12DPP on samples annealed at T_o. The results are shown

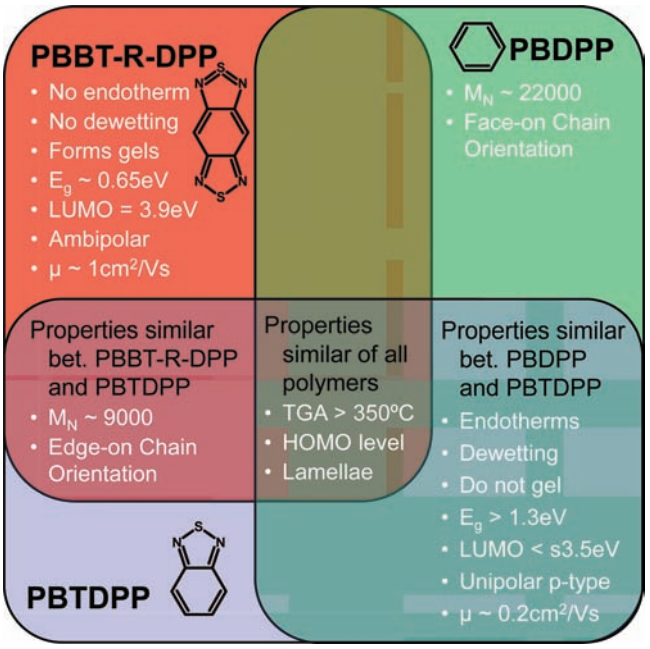

Figure 5. Venn diagram showing properties that are individual to or shared between PBDPP (green), PBTDPP (blue), and the BBT-containing polymers (red). The regions in which the properties are unique to the polymer also contain the chemical structure of the acceptor moiety that was varied.

in Figure 4b. The three curves at the bottom of the figure show the overlap of the raw data for all three polymers, while the top curves are separated arbitrarily for clarity. We observe a peak appearing around 3.5° for PBDPP, implying that a similar lamellar structure observed for PBTDPP and PBBTDPP is instead found in plane, with the polymer chains in a face-on orientation. Apart from this, no other defined peaks were observed, implying that little in-plane order exists for PBTDPP and PBBT-12DPP. In conclusion, XRD measurements show that PBDPP chains take on a face-on configuration, whereas PBTDPP and PBBT12DPP take on a edge-on configuration. In addition, the lack of other peaks imply that there no other types of ordering can be observed, including π-stacking.

■ DISCUSSION

In order to synthesize higher performing polymers, we need to identify and understand the factors that affect transistor performance. We begin with a comparison of the measured properties in order to correlate them with changes in acceptor moiety used. Overall, the three polymers share some similar properties, including chemical stability, HOMO levels, the formation of lamellae (though with different chain orientations). While properties other than the aforementioned were shown to vary between polymers, we do not observe a gradual transition of properties with the different acceptor moieties used. Instead, we find a stark contrast between the BBT-containing polymers and the other polymers, as summarized in a Venn diagram in Figure 5.

Despite differences in ordering and molecular weight, PBDPP and PBTDPP are remarkably similar in terms of electronic and physical properties, which in turn affect transistor behavior. Electronically, both materials have low-lying LUMOs as well as bandgaps more than twice those of the BBT-containing polymers. Both these properties prevent effective injection of n-type charges, resulting in PBDPP and having weak or nonexistent n-type transport. Physically, good solubility and the coincidence of dewetting with endotherms appearing in DSC indicate that the solubilizing side groups most likely have determining effects on the thermo-mechanical properties of PBDPP and PBTDPP. These shared physical properties of PBDPP and PBTDPP affect the stability of transistor performance at different annealing temperatures. Annealing at temperatures at or beyond the endotherms causes the polymer films to dewet and break up, destroying transport at higher annealing temperatures. In addition, PBDPP and PBTDPP share similar transistor performance in terms of mobilities, both around 0.2 $cm^2V^{-1}s^{-1}$. However, the differences in molecular weight and chain orientation to the substrate between PBDPP and PBTDPP make correlating their mobilities difficult.

In comparison, the BBT-containing polymers have markedly different properties compared to PBDPP and PBTDPP due to their BBT moiety. The stronger accepting strength of BBT increases the LUMO values substantially and lowers the HOMO slightly, resulting in bandgaps less than half of those of PBDPP and PBTDPP. With increased LUMO and decreased HOMO values, injection of n-type and p-type charges occurs more easily and the polymers are strongly ambipolar. In terms of physical properties, the BBT-containing polymers show no endotherms, have poor solubility, form gels in solution easily and do not dewet during annealing The most likely reasons that can explain the intractability of the polymers are high molecular weight, interchain interactions and structural ordering (which prevents the chains from moving freely), or a combination thereof. The effect of molecular weight can be excluded as the BBT-polymers have the lowest molecular weights of the family. The increase in structural ordering with annealing for PBBT12DPP also shows that the polymer chains are not locked into ordered structures in the as-cast film and are tractable enough to align themselves. Coupled with the strong planarity of the accepting moieties to the polymer backbone, the effect of side groups on the thermo-mechanical properties should predominate, as it does for PBDPP and PBTDPP. We therefore conclude that interchain interactions most likely play a dominant role in determining the physical properties of BBT-containing polymers. Hence, BBT-containing polymer transistors are able to operate despite high annealing temperatures as the film integrity is maintained via interchain binding.

Interchain interactions may also play an important role explaining the difference in mobility among the polymers. While the differences in molecular weight and chain orientation between PBDPP and PBBT12DPP make correlating mobilities difficult, PBTDPP and PBBT12DPP are remarkably similar in terms of molecular weight. We observe that apart from the difference in the acceptor moiety used, the repeat unit lengths and the solubilizing side groups are the same. The two polymers are similar in terms of molecular weight (~9kD) and structural ordering (edge-on chain orientation, no observable π-stacking). In fact, PBTDPP exhibits higher ordering than PBBT12DPP at all annealing temperatures. Despite that, PBTDPP consistently has lower mobility than PBBTDPP. The above observations leave interchain interactions between the polymers as the most probable cause of the higher thermal stability, lower solubility and better transport properties of PBBT12DPP as compared to PBTDPP. The probable mechanisms by which the BBT moiety can contribute to stronger interchain interactions are stronger

interchain donor−acceptor (DA) interactions[3c,e,14] and S−N intermolecular contact effects from the BBT moiety.[15]

CONCLUSION

We have studied the electronic, physical and transistor properties of a family of donor−acceptor polymers consisting of diketopyrrolopyrrole (DPP) coupled with different accepting companion units in order to determine the effects of donor−acceptor interaction. Using the electronically neutral benzene (B), the weakly accepting benzothiadiazole (BT) and the strongly accepting benzobisthiadiazole (BBT), the accepting strength of the companion unit was systematically modulated without any change in either the length or structure of the conjugated backbone of the repeat unit, or in solubilizing groups used. We observe that intrachain donor−acceptor interactions are complex, with interacting moieties taking on donor and/or acceptor roles depending on their relative energy levels. In particular, we find that the BBT moiety, rather than DPP, takes on the role of the acceptor when paired.

DPP, coupled with the strong acceptor BBT, results in the strongly ambipolar PBBT6DPP and PBBT12DPP, with equivalent p-type and n-type mobilities above 0.5 $cm^2V^{-1}s^{-1}$. In particular, PBBT12DPP has mobilities exceeding 1 $cm^2V^{-1}s^{-1}$. For PBTDPP and PBDPP, in which DPP is coupled to the weaker acceptor BT and the electronically neutral B respectively, we observe only p-type unipolar transport. Nonetheless mobilities for both polymers are around 0.2 $cm^2V^{-1}s^{-1}$. The performances of PBDPP and PBTDPP transistors degraded quickly after annealing beyond 200 °C. In contrast, transistors fabricated with BBT-containing polymers are very thermally stable, with mobilities remaining above 0.1 $cm^2V^{-1}s^{-1}$ even when the samples are annealed up to 300 °C. This is because the BBT moiety has a strong effect on interchain interactions. In turn, interchain interactions enable higher thermal stability and higher performance for transistors with BBT-containing polymers as the active layer.

ASSOCIATED CONTENT

Supporting Information. Experimental details, chemical structure of the acceptor monomers (Figure S1), TGA data for all polymers (Figure S2), DSC data for all polymers (Figure S3), comparison of the fluidity of the polymer solutions (Figure S4), transistor properties of PBBT6DPP (Figure S5), optical micrographs of the polymer films at different annealing temperatures (Figure S6), air stability experiments of PBBT12DPP (Figure S7), and full citation list with complete author list. This material is available free of charge via the Internet at http://pubs.acs.org.

AUTHOR INFORMATION

Corresponding Author

*wudl@chem.ucsb.edu; ajhe@physics.ucsb.edu

Author Contributions

‖These authors contributed equally.

ACKNOWLEDGMENT

Support for research was provided by the Air Force Office of Scientific Research (Charles Lee, Program Officer), the National Science Foundation Polymer program (Grant No. NSF-DMR-0856060) and by the Korean Ministry of Science via a Global Research Laboratory (GRL) award. Partial Support by DARPA through CBRITE Corporation is gratefully acknowledged. Support for J.F. through the Center for Energy Efficient Materials (CEEM) supported by the DOE as an EFRC. A portion of this work was done in the UCSB nanofabrication facility, part of the NSF funded NNIN network. J.D.Y. thanks G. Hernandez-Sosa, S. Valouch, N. Banerji, C. Takacs, and J.H. Seo for useful discussions. J.F. thanks M.F. Wang and W.B. Cui for technical assistance and useful discussions.

REFERENCES

(1) (a) Zhang, Q.; Tour, J. *J. Am. Chem. Soc.* **1997**, *119*, 5065–5066. (b) Zhang, Q.; Tour, J. *J. Am. Chem. Soc.* **1998**, *120*, 5355–5362. (c) Jenekhe, S.; Lu, L.; Alam, M. *Macromolecules* **2001**, *34*, 7315–7324. (d) Cheng, Y.; Yang, S.; Hsu, C. *Chem. Rev.* **2009**, *109*, 5868–5923.

(2) (a) Usta, H.; Facchetti, A.; Marks, T. *J. Am. Chem. Soc.* **2008**, *130*, 8580–8581. (b) Liu, J.; Zhang, R.; Osaka, I.; Mishra, S.; Javier, A. E.; Smilgies, D.; Kowalewski, T.; McCullough, R. D. *Adv. Funct. Mater.* **2009**, *19*, 3427–3434. (c) Kim, D. H.; Lee, B.; Moon, H.; Kang, H. M.; Jeong, E. J.; Park, J.; Han, K.; Lee, S.; Yoo, B. W.; Koo, B. W.; Kim, J. Y.; Lee, W. H.; Cho, K.; Becerril, H. A.; Bao, Z. *J. Am. Chem. Soc.* **2009**, *131*, 6124–6132. (d) Guo, X.; Kim, F. S.; Jenekhe, S. A.; Watson, M. D. *J. Am. Chem. Soc.* **2009**, *131*, 7206–7207. (e) Guo, X.; Ortiz, R. P.; Zheng, Y.; Hu, Y.; Noh, Y.; Baeg, K.; Facchetti, A.; Marks, T. J. *J. Am. Chem. Soc.* **2011**, *133*, 1405–1418.

(3) (a) Yan, H.; Chen, Z.; Zheng, Y.; Newman, C.; Quinn, J.; Dotz, F.; Kastler, M.; Facchetti, A. *Nature* **2009**, *457*, 679–686. (b) Zhang, W.; Smith, J.; Watkins, S. E.; Gysel, R.; McGehee, M.; Salleo, A.; Kirkpatrick, J.; Ashraf, S.; Anthopoulos, T.; Heeney, M.; McCulloch, I. *J. Am. Chem. Soc.* **2010**, *132*, 11437–11439. (c) Tsao, H. N.; Cho, D. M.; Park, I.; Hansen, M. R.; Mavrinskiy, A.; Yoon, D. Y.; Graf, R.; Pisula, W.; Spiess, H. W.; Müllen, K. *J. Am. Chem. Soc.* **2011**, *133*, 2605–2612. (d) Bronstein, H. *J. Am. Chem. Soc.* **2011**, *133*, 3272–3275. (e) Li, Y.; Sonar, P.; Singh, S. P.; Soh, M. S.; van Meurs, M.; Tan, J. *J. Am. Chem. Soc.* **2011**, *133*, 2198–2204.

(4) (a) Allard, S.; Forster, M.; Souharce, B.; Thiem, H.; Scherf, U. *Angew. Chem., Int. Ed.* **2008**, *47*, 4070–4098. (b) Gelinck, G.; Heremans, P.; Nomoto, K.; Anthopoulos, T. D. *Adv. Mater.* **2010**, *22*, 3778–3798.

(5) (a) Letizia, J.; Salata, M.; Tribout, C.; Facchetti, A.; Ratner, M.; Marks, T. *J. Am. Chem. Soc.* **2008**, *130*, 9679–9694. (b) Mondal, R.; Miyaki, N.; Becerril, H.; Norton, J.; Parmer, J.; Mayer, A.; Tang, M.; Brédas, J.; McGehee, M.; Bao, Z. *Chem. Mater.* **2009**, *21*, 3618–3628. (c) Kim, F.; Guo, X.; Watson, M.; Jenekhe, S. *Adv. Mater.* **2010**, *22*, 478–482.

(6) Yuen, J. D.; Kumar, R.; Zakhidov, D.; Seifter, J.; Lim, B.; Heeger, A. J.; Wudl, F. *Adv. Mater.* **2011**, *23*, 3780–3785.

(7) (a) Bürgi, L.; Turbiez, M.; Pfeiffer, R.; Bienewald, F.; Kirner, H.; Winnewisser, C. *Adv. Mater.* **2008**, *20*, 2217–2224. (b) Bijleveld, J.; Zoombelt, A.; Mathijssen, S.; Wienk, M.; Turbiez, M.; de Leeuw, D.; Janssen, R. *J. Am. Chem. Soc.* **2009**, *131*, 16616–16617. (c) Sonar, P.; Singh, S. P.; Li, Y.; Soh, M. S.; Dodabalapur, A. *Adv. Mater.* **2010**, *22*, 5409–5413. (d) Bijleveld, J. C.; Gevaerts, V. S.; Di Nuzzo, D.; Turbiez, M.; Mathijssen, S. G. J.; de Leeuw, D. M.; Wienk, M. M.; Janssen, R. A. J. *Adv. Mater.* **2010**, *22*, E242–E246. (e) Bijleveld, J. C.; Verstrijden, R. A. M.; Wienk, M. M.; Janssen, R. A. J. *J. Mater. Chem.* **2011**, *21*, 9224.

(8) (a) Li, Y.; Singh, S.; Sonar, P. *Adv. Mater.* **2010**, *22*, 4862–4866. (b) Nelson, T. L.; Young, T. M.; Liu, J.; Mishra, S. P.; Belot, J. A.; Balliet, C. L.; Javier, A. E.; Kowalewski, T.; McCullough, R. D. *Adv. Mater.* **2010**, *22*, 4617–4621. (c) Li, Y.; Sonar, P.; Singh, S. P.; Soh, M. S.; van Meurs, M.; Tan, J. *J. Am. Chem. Soc.* **2011**, *133*, 2198–2204.

(9) (a) Karikomi, M.; Kitamura, C.; Tanaka, S.; Yamashita, Y. *J. Am. Chem. Soc.* **1995**, *117*, 6791–6792. (b) Kitamura, C.; Tanaka, S.; Yamashita, Y. *Chem. Mater.* **1996**, *8*, 570–578. (c) Bundgaard, E.; Krebs, F. C. *Macromolecules* **2006**, *39*, 2823–2831. (d) Qian, G.; Wang, Z. Y. *Can. J. Chem.* **2010**, *88*, 192–201. (e) Zhang, X.; Steckler, T. T.; Dasari, R. R.;

Ohira, S.; Potscavage, W. J.; Tiwari, S. P.; Coppee, S.; Ellinger, S.; Barlow, S.; Bredas, J.; Kippelen, B.; Reynolds, J. R.; Marder, S. R. *J. Mater. Chem.* **2010**, *20*, 123–134. (f) Mikroyannidis, J.A.; Tsagkournos, D.V.; Sharma, S.S.; Vijay, Y.K.; Sharma, G.D.; , *J. Mater. Chem.* 2011.

(10) Steckler, T. *J. Am. Chem. Soc.* **2009**, *131*, 2824–2826.

(11) (a) Meijer, E.; de Leeuw, D.; Setayesh, S.; van Veenendaal, E.; Huisman, P.; Blom, J.; Hummelen, U.; Scherf, T. Klapwijk *Nat. Mater.* **2003**, *2*, 678–682. (b) Zaumseil, J.; Sirringhaus, H. *Chem. Rev.* **2007**, *107*, 1296–1323.

(12) (a) Sirringhaus, H.; Brown, P. J.; Friend, R. H.; Nielsen, M. M.; Bechgaard, K.; Langeveld-Voss, B. M. W.; Spiering, A. J. H.; Janssen, R. A. J.; Meijer, E. W.; Herwig, P.; de Leeuw, D. M. *Nature* **1999**, *401*, 685–688. (b) Surin, M.; Leclére, P.; Lazzaroni, J.; Yuen, J. D.; Wang, G.; Moses, D.; Heeger, A. J.; Cho, S.; Lee, K. *J. Appl. Phys.* **2006**, *100*, 033712. (c) Kline, R. J.; McGehee, M. D.; Toney, M. F. *Nat. Mater.* **2006**, *5*, 222–228. (d) McCulloch, I.; Heeney, M.; Bailey, C.; Genevicius, K.; MacDonald, I.; Shkunov, M.; Sparrowe, D.; Tierney, S.; Wagner, R.; Zhang, W.; Chabinyc, M. L.; Kline, R. J.; McGehee, M. D.; Toney, M. F. *Nat. Mater.* **2006**, *5*, 328–333. (e) Li, Y.; Wu, Y.; Liu, P.; Birau, M.; Pan, H.; Ong, B. *Adv. Mater.* **2006**, *18*, 3029–30. (f) Fong, H. H.; Pozdin, V. A.; Amassian, A.; Malliaras, G. G.; Smilgies, D.; He, M.; Gasper, S.; Zhang, F.; Sorensen, M. *J. Am. Chem. Soc.* **2008**, *130*, 13202–13203. (g) Kim, D. H.; Lee, B.-L.; Moon, H.; Kang, H. M.; Jeong, E. J.; Park, J.-I.; Han, K.-M.; Lee, S.; Yoo, B. W.; Koo, B. W.; Kim, J. Y.; Lee, W. H.; Cho, K.; Becerril, H. A.; Bao, Z. *J. Am. Chem. Soc.* **2009**, *131*, 6124–6132.

(13) Manuscript submitted.

(14) Rieger, R.; Enkelmann, V.; Müllen, K. *Materials* **2010**, *3*, 1904–1912.

(15) (a) Ono, K.; Tanaka, S.; Yamashita, Y. *Angew. Chem., Int. Ed.* **1994**, *33*, 1977–1979. (b) Yamashita, Y.; Tomura, M. *J. Mater. Chem.* **1998**, *8*, 1933–1944. (c) Cozzolino, A. F.; Vargas-Baca, I.; Mansour, S.; Mahmoudkhani, A. H. *J. Am. Chem. Soc.* **2005**, *127*, 3184–3190. (d) Pang, H.; Vilela, F.; Skabara, P. J.; McDouall, J. J. W.; Crouch, D. J.; Anthopoulos, T. D.; Bradley, D. D. C.; de Leeuw, D. M.; Horton, P. N.; Hursthouse, M. B. *Adv. Mater.* **2007**, *19*, 4438–4442.